PNAS
www.pnas.org

Supplementary Information for

SERF engages in a fuzzy complex that accelerates primary nucleation of amyloid proteins

Ben A. Meinen[a,b], Varun V. Gadkari[c], Frederick Stull[a,b], Brandon T. Ruotolo[c] & James C. A. Bardwell[a,c,*]

[a]Department of Molecular, Cellular, and Developmental Biology, University of Michigan, 1105 N. University Ave., Ann Arbor, MI 48109-1085, USA. [b]Howard Hughes Medical Institute, University of Michigan, 1105 N. University Ave., Ann Arbor, MI 48109-1085, USA.
[c]Department of Chemistry, University of Michigan, 930 N. University Ave., Ann Arbor, MI 48109-1055, USA.

corresponding author: James C. A. Bardwell
Email: jbardwel@umich.edu

This PDF file includes:

www.pnas.org/cgi/doi/10.1073/pnas.1913316116

Supplementary Information Text

Material and Methods

Protein expression and purification. The amino acid sequence (MARGNQRDLARQKNLKKQKDMAKNQKKSGDPKKRMESDAEILRQKQAAADA RREAEKLEKLKAEKTRR) of the *S. cerevisiae* SERF protein (ScSERF), previously known as YDL085C-A, was codon optimized for protein expression in *Escherichia coli,* and the corresponding DNA sequence was synthesized using the tool and service provided by Integrated DNA Technologies. The sequence was ligated into a pET28 vector (provided by the Ming Lei lab at the University of Michigan) with sequences encoding a 6-His-SUMO tag fusion to the N terminus (1). This vector was constructed to enable the simple and scarless removal of the His-SUMO tag by ubiquitin-like-specific protease 1 (ULP1). The plasmid was transformed into *E. coli* BL21 (DE3) cells for protein expression. Cells were grown with shaking at 180 rpm at 37 °C to early log phase in protein expression media that contained 100 μg/ml kanamycin and then shifted to 20 °C. ScSERF expression was then induced by addition of 0.1 mM isopropyl β-D-1-thiogalactopyranoside (IPTG). After 16 h of expression, cells were pelleted by centrifugation and resuspended in lysis buffer containing 40 mM Tris, 10 mM NaP, 10% glycerol, pH. 8.0; 2 tablets of protease inhibitor cocktail were then added (complete mini EDTA-free, Roche).

Cells were lysed using a French press for 3 cycles at 1300 psi. After centrifugation for 30 min at 37,500 *g*, the supernatant was recentrifuged using the same protocol and filtered with a 0.25 μm filter. The filtered cell lysate was

loaded on a 5 ml NiNTA pre-packed column (GE Healthcare, #17524802), and the column was washed with 50 ml of lysis buffer that also contained 10 mM imidazole. The His-SUMO-ScSERF fusion protein was eluted with 20 mM of lysis buffer supplemented with 500 mM imidazole. ULP1 and 10 µl β-mercaptoethanol were added to the eluted material and dialyzed against 40 mM Tris, 300 mM NaCl (pH 8) overnight in the cold room for cleavage and buffer exchange.

The cleaved His-SUMO tag was removed by a second NiNTA column equilibrated with dialysis buffer, and the tag-free cleaved ScSERF product was collected in the column flow-through. The flow-through was concentrated by a 3 K cutoff device (AMICON, #UF900396) and diluted with anion exchange buffer (50 mM Na phosphate, 125 mM NaCl, pH 6). The protein was passed over a 5 ml anion exchange column (HiTrap SP; GE Healthcare, #17115201). The proteins were eluted with a linear gradient of 20 CV with ion exchange buffer supplemented with 1 M NaCl. The elution fractions from the HiTrap column that contained ScSERF as determined by SDS-PAGE were combined, concentrated, and loaded on a 120 ml gel filtration column (HiLoad 16/60 Superdex S75; GE Healthcare, #17106801), followed by elution with 40 mM Hepes, 300 mM NaCl (pH 7.5). Fractions containing ScSERF were pooled, and the ScSERF concentration was determined with the Pierce BCA (Bicinchoninic acid) protein assay (Thermo Scientific). Samples were aliquoted and stored at −80 °C. Point mutations in ScSERF, A63C, or L9W were generated with specific primers (see Supplementary Table 2) using site-directed mutagenesis with a QuickChange Kit

(Agilent). These ScSERF variants were purified following the same protocol that was used for wild-type ScSERF.

Purification of Aβ40. Aβ40 (MDAEFRHDSGYEVHHQKLVFFAEDVGSNKGAIIGLMVGGVV) with an additional N-terminal methionine was purified as previously described (2). The Aβ40 expression vector pETSaC-Aβ40 was kindly provided by Dr. Sheena Radford, University of Leeds.(2) This plasmid was transformed into *E. coli* BL21 (DE3) cells and the protein was induced by 1 mM IPTG for 4 h at 37 °C in LB media. In brief, the purification involves the sonication of induced *E. coli* cells followed by the solubilization of the inclusion bodies that contain Aβ40 in 8 M urea. The Aβ40 protein was purified in a batch mode with DEAE cellulose resin (GE Healthcare). The elution fractions containing Aβ40 were pooled, dialyzed against 50 mM ammonium bicarbonate buffer (pH 7.8), and lyophilized. The samples were then resuspended in 7 M guanidinium chloride (GdnHCl), 50 mM Tris (pH 8) buffer, and aggregates were removed by gel filtration on a preparative S75 column Superdex S75 HiLoad 16/60 followed by another lyophilizing and a polishing step on an analytical Superdex S75 10/300 GL (GE Healthcare, #17517401). This process yields pure and monomeric Aβ40 peptide. Aβ40 was stored lyophilized at −80 °C.

Purification of α-synuclein. The purification of α-synuclein was done as described previously(3). In brief, α-synuclein was expressed from a pET7-7 vector plasmid transformed into *E. coli* strain BL21 (DE3). Protein expression

was induced with 1 mM IPTG for 4 h after the OD of the culture reached 0.6 in LB media. The induced cells were pelleted at 4,000 rpm and resuspended in 25 ml lysis buffer (10 mM Tris, 1 mM EDTA, pH 8). The lysed cells were then boiled at 95 °C for 15–20 min and centrifuged at 11,000 rpm for 20 min. The supernatant was mixed with 10% (w/v) streptomycin sulphate solution (136 μl/ml) and glacial acetic acid (228 μl/ml), and nucleic acids in the pellet were removed by centrifugation at 13,500 × *g* for 30 min. An equal volume of saturated ammonium sulphate was added to the supernatant and incubated at 4 °C for 1 h with intermittent mixing. The precipitated protein was separated by centrifuging it at 13,500 × *g* for 30 min.

The pellet was resuspended in 10 mM Tris-HCl, pH 7.5, and NaOH was used to readjust the pH of the suspension to 7.5. The solution was then dialyzed against 10 mM Tris-HCl pH 7.5, 50 mM NaCl. The protein solution was filtered and loaded onto two 5 ml HiTrap Q HP columns (GE Healthcare, #17115401). The columns were washed with 15 column volumes of 10 mM Tris-HCl, pH 7.5, 50 mM NaCl, and the protein was eluted using a linear gradient to 500 mM NaCl. α-synuclein-containing fractions were pooled, concentrated, and dialyzed against 20 mM K phosphate, pH 7.5 at 4 °C overnight. Aliquots of the protein were prepared, lyophilized, and stored at −80 °C.

ThT aggregation kinetics. To achieve reproducible Aβ40 kinetics, it is crucial to start with pure monomeric Aβ40. Therefore, the assay was conducted as previously described(4). Monomeric Aβ40 was dissolved in 7 M GdnHCl, 50 mM

Tris (pH 8) buffer and loaded on to an analytical Superdex S75 10/300 column (GE Healthcare, #17517401). The center fractions of the monomer peak (13.5 ml elution volume) were collected and iced. The protein concentration was determined by using an extinction coefficient ε 280 = 1490 $M^{-1}cm^{-1}$. The Aβ40 protein typically had a concentration of 80–160 μM at this step.

ScSERF (YDL085C-A) was buffer exchanged into the assay buffer (20 mM NaPi 200 μM EDTA, pH 7.4) via a PD10 desalting column (GE Healthcare). Samples were prepared in low-binding Eppendorf tubes on ice, using careful pipetting to avoid air bubbles. ThT was added to a final concentration of 100 μM from a 10 mM ThT stock. Each sample was then pipetted into multiple wells in 3–4 technical replicates into a 96-well plate that featured low-binding PEG coating (Corning, #3881), 90 μl per well. The plate was sealed with an adhesive sealing sheet (Thermo Scientific, #125434).

Aβ40 amyloid formation assays were initiated by placing the 96-well plate at the specified temperature of 37 °C in a Tecan Infinite M200 plate reader while reading the ThT fluorescence from the bottom using an excitation wavelength of 440 nm and an emission wavelength of 482 nm. Measurements were taken every 5 min under quiescent conditions, and shaking only occurred for 10 s before the fluorescence reading took place. The formation of fibrils was confirmed by TEM.

Immediately prior to performing α-synuclein amyloid formation assays, preexisting aggregates/amyloids and multimers were removed from the α-synuclein preparation by first resuspending the lyophilized α-synuclein in 7 M

GdnHCl, 50 mM Tris (pH 8) buffer and loading the dissolved α-synuclein onto an analytical Superdex S75 10/300 GL column (GE Healthcare, #17517401). α-synuclein was eluted using assay buffer (20 mM NaPI, pH 7.4, 50 mM NaCl, 200 μM EDTA); monomeric α-synuclein was collected, and its concentration was determined by using an extinction coefficient ε 280 = 5600 $M^{-1}cm^{-1}$. A 320 μl stock solution sufficient to allow for 3 technical replicates was prepared by diluting monomeric α-synuclein to the stated concentrations in assay buffer (20 mM NaPI, pH 7.4, 50 mM NaCl, 200 μM EDTA) in low-binding Eppendorf tubes on ice; ThT was added to 25 μM final concentration. 100 μl technical replicates were pipetted into multiple wells of a 96-well microtiter plate with a clear bottom (Corning, #3631). Two glass beads were added per reaction well to accelerate the amyloid formation. The plate was sealed with an adhesive sealing sheet (Thermo Scientific). Assays were initiated by placing the 96-well plate at 37 °C in a Tecan Infinite M200 plate reader while reading the ThT fluorescence from the bottom using an excitation wavelength of 440 nm and an emission wavelength of 482 nm. Measurements were taken every 10 min under constant shaking at 300 rpm. The formation of fibrils was confirmed by TEM.

Kinetic data analysis. The experimental data were normalized so that the relative mass concentration of aggregates was 0 at time 0 and 1 at the completion of the aggregation. Kinetic data were normalized and fitted using the platform on AmyloFit (https://www.amylofit.ch.cam.ac.uk/login) (4). The formula for normalizing the data was

$$y_{norm,i} = \left(1 - M_{0,\mathrm{frac}}\right)\frac{y_i - y_{\mathrm{baseline}}}{y_{\mathrm{plateau}} - y_{\mathrm{baseline}}} + M_{0,\mathrm{frac}}$$

where y_i is the signal at any time point, $y_{baseline}$ is the average baseline fluorescence signal, $y_{plateau}$ is the average fluorescence value of the data point after the plateau is reached, and $M_{0,frac}$ is the relative initial concentration of aggregates between time point 0 and the completion of the aggregation in the original data. The halftime is the point where the fluorescence signal has reached half of the plateau value. The halftimes were determined by fitting a straight line to the fluorescent data points that lie between 0.3 and 0.7 fraction where 0 is baseline and 1.0 is the plateau fluorescence. The point at which this line crosses the value of 0.5 is taken as the halftime.

Aggregation traces of 25 μM Aβ40 with different concentrations of ScSERF in molar ratios of 0 to 100% were analyzed by a kinetic nucleation model that is defined by a set of microscopic rate constants, one for primary nucleation (k_n), one for secondary nucleation (k_2), and one for fibril elongation (k_+) (5, 6) In the case of unseeded aggregation, the system depends only on the combination of the rate constants for primary nucleation k_+k_n and secondary nucleation k_2k_+, not on the individual rate constants.

To determine the nucleation model, the halftimes of different initial monomer concentrations m_0 in the absence or presence of 1:0.2 molar ratio ScSERF were determined. In both cases, a double logarithmic plot showed a slight positive curvature as previously described for Aβ40, indicating a multi-step secondary nucleation model (4, 6). The kinetics were fitted by keeping the reaction orders for primary and secondary nucleation at the Aβ40 values $n_c = n_2 = 2$. The combined rate constants for primary nucleation and secondary nucleation were

the only free fitting parameters. The web tool (AmyloFit) defines the multi-step secondary nucleation mechanism as follows(4, 7)

$$\frac{dP}{dt} = k_2 M(t) \frac{m(t)^{n2}}{1 - \frac{m(t)^{n_2}}{K_M}} + k_n m(t)^{n_c}$$

$$\frac{dM}{dt} = 2\left(k_+ m(t) - k_{off}\right) P(t)$$

where $k_2 = \frac{\overline{k_2}}{K_M}$ and $K_M = \frac{k_b + \bar{k}_2}{k_f}$. Here, m_0 is the initial monomer concentration, M_0 is the initial fibril mass concentration, P_0 is the initial fibril number concentration, k_n is the primary nucleation rate constant, n_c is the critical nucleus size for primary nucleation (2), n_2 is the critical nucleus size for secondary nucleation (2), K_M is the Michaelis-Menten constant, which determines the monomer concentration at which secondary nucleation begins to saturate, and k_+ is the elongation rate constant. The integrated rate law for the normalized aggregate mass concentration is determined as (4, 6)

$$\frac{[M]}{[M]_\infty} = 1 - \left(1 - \frac{[M]_0}{[M]_\infty}\right) e^{-k_\infty t} * \left(\frac{B_- + C_+ e^{kt}}{B_+ + C_+ e^{kt}} * \frac{B_+ C_+}{B_- C_+}\right)^{\frac{k_\infty}{\overline{\kappa k}_\infty}}$$

where the definitions of the parameters are

$$\kappa = \sqrt{2[m]_0 k_+ \frac{[m]_0^{n_2} k_2}{1 + [m]_0^{n_2}/K_M}}$$

$$\lambda = \sqrt{2 k_+ k_n [m]_0^{n_c}}$$

$$C_\pm = \frac{k_+ [P]_0}{k} \pm \frac{k_+ [M]_0}{2[m]_0 k_+} \pm \frac{\lambda^2}{2\kappa^2}$$

$$k_\infty = 2k_+[P]_\infty$$

$$\bar{k}_\infty = \sqrt{k_\infty^2 - 2C_+C_-k^2}$$

$$k_\infty = \sqrt{(2k_+P(0))^2 - 2A - 4k_+k_2m_{tot}K_M\frac{\log[K_M]}{n_2}}$$

$$A = \frac{2k_+k_nm_0^{n_c}}{n_c} - 2\,k_+k_2m_{tot}K_M\frac{log[K_M]}{n_2} - 2k_+k_2K_Mm_0({}_2F_1\left[\frac{1}{n_2}, 1{,}1 + \frac{1}{n_2}, -\frac{m_0^{n_2}}{K_M}\right] - 1)$$

$$B_\pm = \frac{k_{\infty\pm}\bar{k}_\infty}{2\kappa}$$

Preparation of Aβ40 seeds and α-synuclein seeds. Monomeric Aβ40 was prepared as described above and Aβ40 seed fibrils were formed in 96-well plates with low-binding PEG coating (Corning, #3881). ThT was added to one sample and the ThT fluorescence signal was monitored to assure the plateau fluorescence was reached in the other ThT-free wells. The pre-formed Aβ40 fibrils from these ThT-free wells were used directly for the anisotropy experiments shown in Supplementary Fig. 4. To generate Aβ40 seeds for the kinetic experiments shown in Fig. 2, the pre-formed Aβ40 fibrils were sonicated for 10 min in a sonication bath (Branson, #1510). The concentration of seeds was based on the initial monomeric concentration used. Seeded ThT kinetics experiments were prepared as described above (ThT aggregation kinetics) with the addition of the indicated seed concentration to the reaction mixture. Seed fibrils were produced from monomeric α-synuclein by polymerizing 300 μl of a monomeric α-synuclein solution in a concentration range of 300–800 μM by

incubating for 3 days at 40 °C with 500 rpm shaking in a low-binding Eppendorf tube. These α-synuclein fibrils were then converted into seeds by sonicating them for 10 min in a sonication bath (Branson, #1510) and used for the seeded ThT kinetics experiments shown in Fig. 2. Seeded ThT kinetics experiments were performed as described for the non-seeded reactions except that the seeded α-synuclein experiments were not shaken continuously but rather performed under quiescent conditions in Corning #3881 plates with shaking only before measuring the fluorescence.

Protein labeling with Alexa Fluor 532. The labeling of the primary amines present in Aβ40 was done with Alexa Fluor 532 N-hydroxysuccinimide (NHS) ester as described by the manufacturer (Thermo Scientific). In brief, lyophilized monomeric Aβ40 was resuspended in 50 mM sodium bicarbonate buffer (pH 8.3) and the NHS ester dye was resuspended in 100% DMSO. The dye was added to Aβ40 at a 10-fold molar excess and incubated for 1 h at room temperature. Free dye was removed by performing gel filtration on a 120 ml (Superdex S75 10/300 Gl column (GE Healthcare, #17517401) in 50 mM ammonium bicarbonate buffer (pH 7.8).

Labeling of ScSERF (A63C) was performed by first reducing any intermolecular disulfides that had formed between Cys63 residues by incubating in 20 mM Tris buffer pH 8.0,10 mM DTT for 1 h on ice. Excess DTT was removed by gel filtration on a PD10 desalting column (GE Healthcare) into 50 mM Tris, 50 mM NaCl (pH 8.0) with a final elution volume of 3.5 ml protein. ScSERF-A63C was then incubated with 10-fold molar excess of Alexa Fluor 532 (AF532:C-5

maleimide) dye in 50 mM Tris, 50 mM NaCl (pH 8.0). The excess dye was removed by applying the sample to 120 ml size exclusion chromatography (Superdex S75 10/300 GL) (GE Healthcare, #17517401). The fractions containing the labeled ScSERF were pooled together and concentrated. ScSERF has no aromatic residues to facilitate concentration determination by UV absorption. Therefore, the labeling efficiency was estimated by comparing the protein concentration as determined by BCA with the label content as determined by examining the extinction coefficient of the label ε 528 = 78,000 $M^{-1}cm^{-1}$. By these means, we could estimate the label to protein ratio to be ~0.9.

Fluorescence anisotropy. To determine the dissociation binding constant K_d for monomeric Aβ40 and ScSERF, fluorescence anisotropy was performed. In a 1 ml cuvette at 25 °C, 200 nM AF532-labeled Aβ40 in 20 mM ammonium acetate, pH 7.4, was titrated with a stock (2.2 mM) of ScSERF also in 20 mM ammonium acetate, pH 7.4. The binding between monomeric A63C-labeled ScSERF with AF532 and unlabeled α-synuclein was monitored by fluorescence anisotropy conducted in a similar manner by titrating α-synuclein into 500 nM AF532-labled ScSERFA63C (20 mM ammonium acetate, pH 7.4) at 25 °C.

For the fibril binding experiment, 500 nM AF532-labeled ScSERF was titrated with pre-formed fibrils of Aβ40 or α-synuclein and competed with unlabeled ScSERF (20 mM NaPI, 200 μM EDTA, pH 7.4) at 25 °C.

Anisotropy was calculated according to the following equations

$$G = \frac{I_{hv}}{I_{hh}}$$

$$r = \frac{I_{vv} - GI_{vh}}{I_{vv} + 2GI_{vh}}$$

where *G* is the instrument correction factor, *r* is anisotropy, and *I* is the fluorescence intensity measured with polarizers in the orientations indicated in the subscripts (*v* is vertical and *h* is horizontal). Anisotropy was recorded with a Cary Eclipse Spectrofluorometer (Agilent) using λ_{ex} = 532 nm (5 nm bandpass) and λ_{em} = 552 (10 nm bandpass). The titration data was fitted to the following binding isotherm

$$f_a = \frac{\Delta f_a\,[Ligand_{(ScSERF\ or\ \alpha\mathrm{Syn})}]}{(K_d + [Ligand_{(ScSERF\ or\ \alpha\mathrm{Syn})}])} + f_a 0$$

where f_a is the fluorescence anisotropy signal, Δf_a is the total signal change, $f_a 0$ is the y axis intercept, K_d is the dissociation constant.

Transmission electron microscopy. Aβ40 and α-synuclein at the concentrations indicated in the absence or presence of indicated ScSERF concentrations were incubated as described in the ThT assay section. Samples were taken at the plateau of the ThT kinetic experiments. 5 μl of sample was spotted on a formvar grid with a carbon film and blotted for 5 min. The samples were stained for 1 min with a 1.5% uranyl formate solution. The samples were imaged using either a Tecnai T12 or JEOL JEM-1400(Plus) TEM.

SDS-PAGE analysis. Aβ40 or α-synuclein in the absence or presence of the indicated ScSERF concentrations was prepared as described above (ThT aggregation kinetics). Samples from one well (80 μl) were taken when the ThT

signal had reached the plateau phase. The soluble and insoluble fractions were separated by 60 min centrifugation at 20,000 × *g* using a Beckmann Microfuge 20R. The insoluble fraction was washed once in assay buffer. 10 μl samples were then run on an Invitrogen Novex 16% Tricine Protein Gel followed by Fairbanks Coomassie Blue staining (8). The PAGE was stained in Fairbanks A by first microwaving for 30 s and staining for 30 min. The destaining process took place in Fairbanks C for 1 h and Fairbanks D for 2–16 h until the PAGE was completely destained.

Circular dichroism spectroscopy. To monitor changes in the secondary structure of ScSERF, ScSERF was diluted into 20 mM NaPI pH 7.4, 25 mM NaCl to a final concentration of 0.2 mg/ml. Far-UV CD spectra were taken by scanning from 190 nm to 250 nm in a J-1500 spectrophotometer (Jasco) at the indicated temperatures. The mean residue ellipticity $[\theta]_{mrw,\lambda}$ was calculated as follows

$$[\theta]_{mrw,\lambda} = MRW\ [\theta_\lambda]/10\ d\ c$$

where *MRW* is the mean residue weight, θ_λ is the observed ellipticity (degrees) at wavelength *λ*, *d* is the path length (0.1 cm), and *c* is the concentration in mg/ml.

Kinetics simulation. Aβ40 amyloid kinetics were simulated using the equations previously derived by the Knowles group (9) and the kinetic simulation software Berkley Madonna (https://berkeley-madonna.myshopify.com/). The initial rate constants used for Aβ40 were: primary nucleation rate (k_2) = 2×10^{-6}, elongation

rate (k_4) = 3×10^5, and secondary nucleation rate (k_3) = 3×10^3. The following integrated rate laws and parameters were applied

$$\frac{dP(t)}{dt} = k_1(M(t) - (2n_c - 1) * P(t)) + k_2 x(t)^{nc} + k_3 M(t) m(t)^{n2}$$

$$\frac{dM(t)}{dt} = (k_4 x - n_c(n_c - 1)\frac{k_1}{2})P(t) + n_c k_2 x(t)^{nc} + n_2 k_2 M x(t)^{n2}$$

$$\frac{d(x)}{dt} = -n_c k_2 x^{nc} - n2k_3 M x^{n2} - 2k_4 x P(t)$$

where n = 2, n_c = 2, x = 25 μM Aβ, $M(t)$ = Fibrils mass fraction, $P(t)$ = Total fibril number

Native IM-MS measurements. Native IM-MS experiments were carried out on a Synapt G2 traveling wave ion mobility-mass spectrometer (Waters). Aqueous samples were introduced into the gas phase by a nanoelectrospray ionization (nESI) source operated in positive ion mode. Ions were generated using a capillary voltage of 1100-1200 V and sample cone voltage of 10 V. The instrument was operated with a backing pressure of 2.63 mbar, source pressure of 7.38×10^{-3} mbar, trap pressure of 3.34×10^{-2} mbar, IM pressure of 3.47 mbar, transfer pressure of 1.00×10^{-6} mbar, and time-of-flight (ToF) pressure of 1.44×10^{-6} mbar. The IM wave height was 30 V and the IM wave velocity was 600 m/s.

ScSERF was co-incubated with Aβ40 or α-synuclein to a final concentration of 25 μM each in 20 mM ammonium acetate, pH 7.4. A ThT assay was carried out in these buffer conditions to verify that the aggregation kinetics of Aβ40 was

not changed due to the change in reaction buffer. Samples were incubated at 37 ºC. Time course experiments were conducted by setting up separate reactions that were removed from 37 ºC at the indicated times for IM-MS analysis. All reactions were diluted 2.5-fold to final concentrations of 10 μM prior to IM-MS analysis to prevent nonspecific interactions due to nESI. Although, various substoichiometric ratios of ScSERF to Aβ40/α-synuclein were screened by other methods, a 1:1 ratio was chosen for the IM-MS experiments to ensure that ScSERF bound complexes were sufficiently abundant to be observed. The 1:1 ratio was the highest ratio of ScSERF to Aβ40/α-synuclein where ScSERF was still observed to accelerate aggregation. Thus, we anticipate that the complexes observed at this ratio are representative of those present at substoichiometric ratios.

ATDs were fit to a minimal number of Gaussian functions, and the peak centers of the Gaussian functions were converted to CCSs using a previously described protocol(10). CCS measurements were calibrated using native β-lactoglobulin, ubiquitin, cytochrome C, insulin, melittin, and denatured ubiquitin. Calibration was conducted using a database of known values in helium, and all CCS values reported are an average of at least 3 replicates. The associated least square error with each average CCS combines inherent calibrant error from drift tube measurements (3%), the calibration curve error (R^2), and two times the replicate standard deviation error as per a previously published protocol (11).

The dissociation constant of ScSERF binding to Aβ40 monomer was determined by preparing samples containing 2 μM ScSERF, and 5, 10, 40, and

60 μM of Aβ40 in 20 mM ammonium acetate buffer (pH 7.4). Titration of Aβ40 beyond a final concentration of 60 μM resulted in Aβ40 aggregation, which interfered with the K_d measurement. Each sample was analyzed three times by three separate nESI needles. The three analyses were treated as three technical replicates and plotted separately. The mass spectra were integrated to determine total abundances of free and bound ScSERF. Since the ionization efficiencies of ScSERF and ScSERF:Aβ40 vary significantly, we utilized the response factor R as described previously (57):

$$R = \frac{PL}{P}$$

where PL is the total signal abundance of ScSERF: Aβ40, and P is the abundance of unbound ScSERF. To account for the difference in ionization efficiency the response factor relationship (R/R+1) was plotted agains the corresponding concentration of Aβ40 for all three replicates, and all points were fit to the following nonlinear equation adapted from Ishii et al.

$$\frac{\mathrm{R}}{\mathrm{R}+1} = 0.5 * \frac{K_d}{[\mathrm{ScSERF}]0} * \left[1 + \frac{[\mathrm{ScSERF}]_0}{K_d} + \frac{[\mathrm{A\beta40}]_0}{K_d} - \sqrt{\left(1 + \frac{[\mathrm{ScSERF}]_0}{K_d} - \frac{[\mathrm{A\beta40}]_0}{K_d}\right)^2 + \frac{4[\mathrm{A\beta40}]_0}{K_d}} \right]$$

where $[\mathrm{ScSERF}]_0$ and $[\mathrm{A\beta40}]_0$ are the initial concentrations of the respective species, and K_d is the dissociation constant.

Raw data was analyzed using MassLynx (Waters). ATDs for all CCS calibrants as well as ScSERF complex samples were extracted from raw data using TWIMExtract (12), and ion mobility ATDs were fit to Gaussian functions using CIUSuite2 (13).

Supplementary Figure

Supplementary Figure 1 Sequence alignment of ScSERF
Alignment of S. cerevisase ScSERF protein with representative homologues from a diverse selection of other eukaryotes. The accession codes of the sequences selected from top to bottom are;
Q3E7B7, Q9UTF0, O75920, P84101, Q32P76, Q9BKU8, Q9BKU8, A5JSS4, Q9 VEW2, A6H8S3, A0A3Q2ULA2, P84102, F6Y2S0.

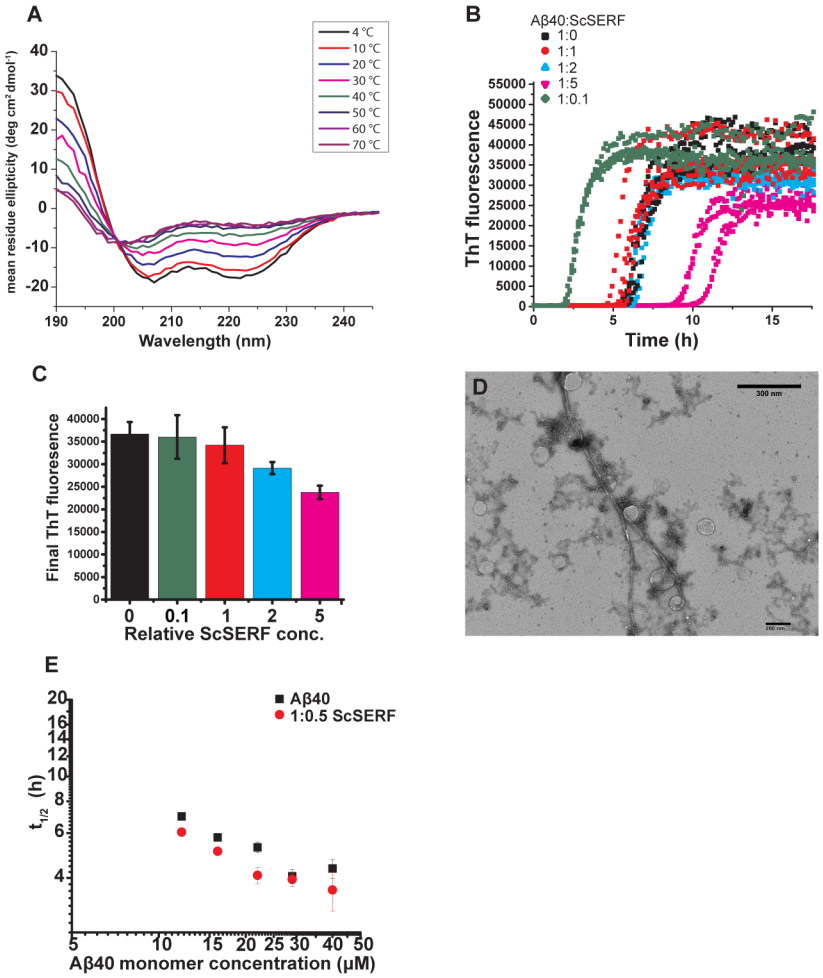

Supplementary Figure 2 Aβ40 amyloid aggregation with high molar excess of ScSERF.
(A) Temperature dependency of ScSERF secondary structure. CD signal of 0.2 mg/ml ScSERF plotted as mean residue ellipticity collected at increasing temperatures. (B) Kinetic assay of 25 μM Aβ40 incubated in the absence (black) or presence of different concentrations of ScSERF measured by ThT fluorescence. (C) Final ThT fluorescence of plateau in dependence of different ScSERF concentrations – average of at least three replicates. (D) representative TEM image of Aβ40 fibrils in the presence of 5 molar excess ScSERF. (E) Double logarithmic plot of average half time of Aβ40 aggregation at higher concentrations than presented in Figure 1 D in the absence (black) or presence of 1:0.5 Aβ40:ScSERF (red).

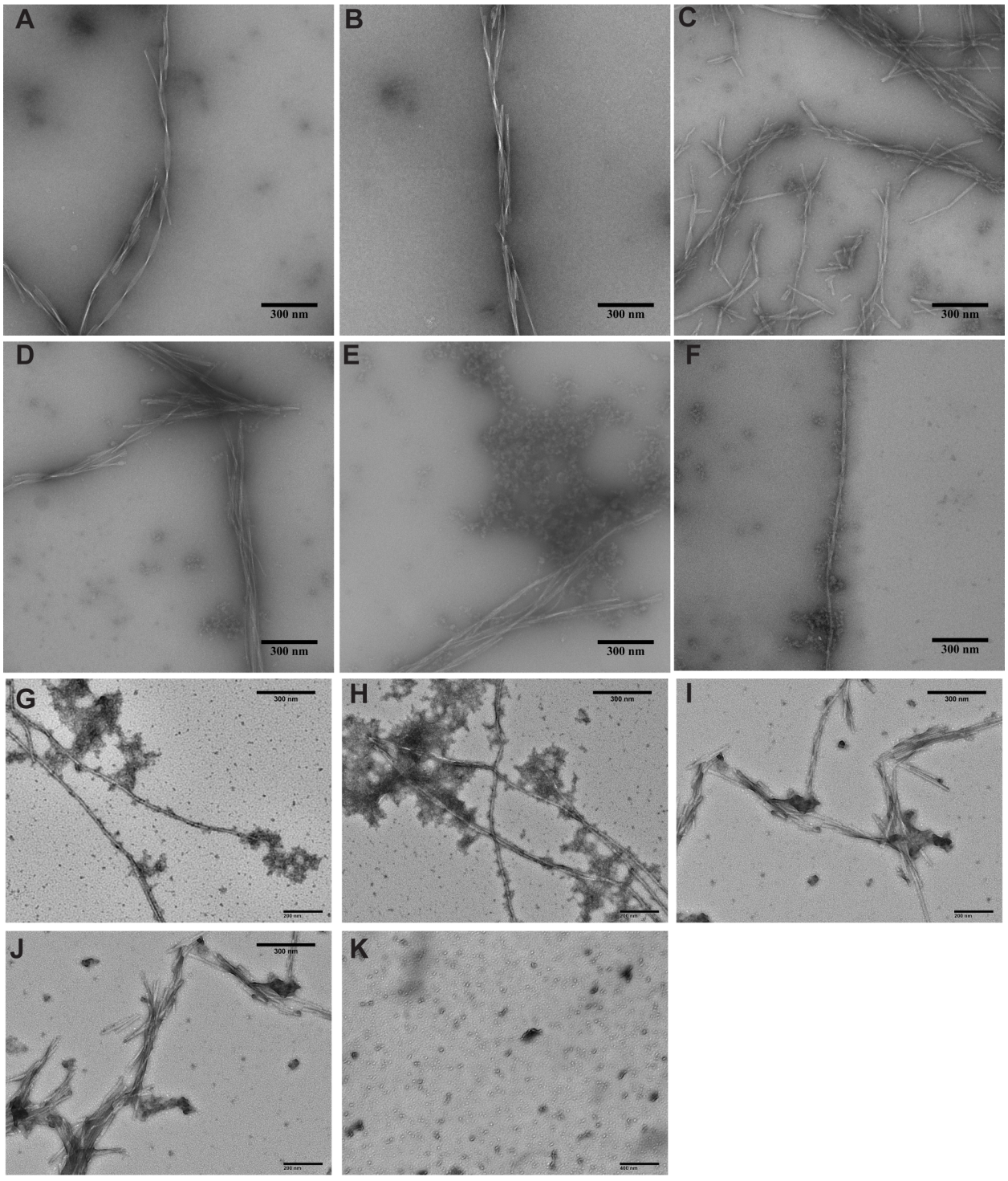

Supplementary Figure 3 Characterization of Aβ40/α-synuclein fibrils +/- ScSERF. Aβ40 was incubated in the presence or absence of different molar ratios of ScSERF for 48 h. Images were taken by TEM. (A,B) Representative images of Aβ40 fibrils.(C,D) Images of Aβ40 fibrils in the presence of 0.1 molar equivalent of ScSERF. (E,F) Images of Aβ40 fibrils in the presence of 1 molar

equivalent of ScSERF. (G,H) Images of 200 μM α-synuclein after completion of the ThT assay. (I,J) Images of 200 μM α-synuclein incubated with 100 μM ScSERF. (K) Image of ScSERF alone, also incubated for the duration of the ThT experiment

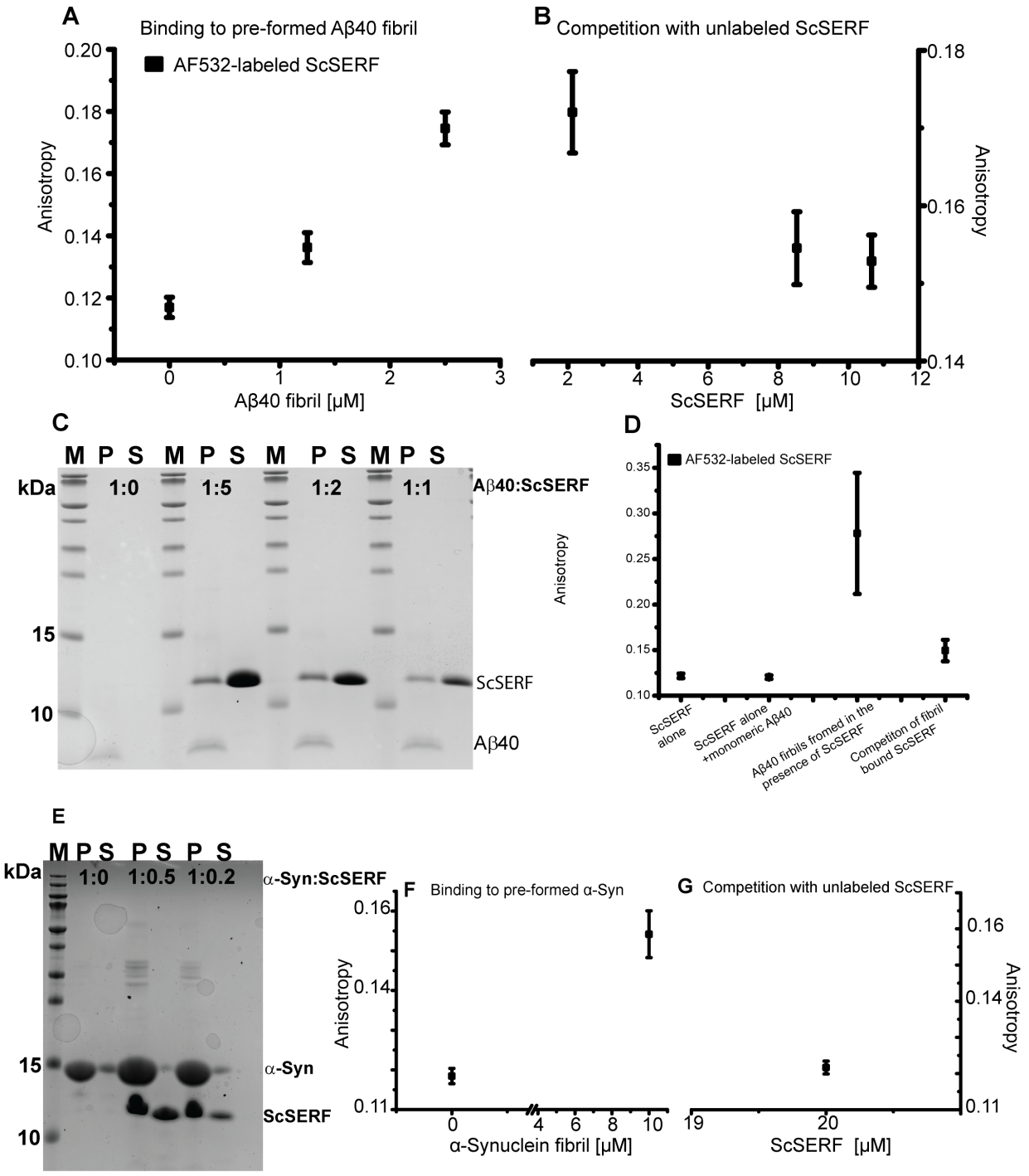

Supplementary Figure 4. ScSERF attachment to Aβ40/α-synuclein fibrils. (A) Fluorescence anisotropy change of AF532-labeled ScSERF upon addition of pre-formed Aβ40 fibrils. (B) Change in anisotropy upon competition with unlabeled ScSERF. Titration was performed at 25 °C (20 mM NaPI, 200 μM EDTA, pH 7.4). (C) SDS-PAGE analysis of soluble (S) and insoluble (P) fractions of 25 μM Aβ40 aggregation at the plateau of aggregation in the presence of different

concentrations of ScSERF: 125 μM (1:5), 50 μM (1:2), and 25 μM (1:1); M: marker, P: pellet, S: soluble fraction. (D) AF532-labeled ScSERF is not integrated into Aβ40 fibrils. Plots show fluorescence anisotropy change of AF532-labeled ScSERF upon addition of monomeric Aβ40, after incubation with Aβ40 for 72 h at 37 °C, and when competed against with unlabeled ScSERF (20 mM NaPI, 200 μM EDTA, pH 7.4, 25 μM ThT). (E) SDS-PAGE analysis of soluble (S) and insoluble (P) fractions of 100 μM α-synuclein aggregation for different ratios of α-synuclein:ScSERF (1:0, 1:0.5, and 1:0.2); M, P, and S same as in (C). (F,G) Fluorescence anisotropy change of AF532-labeled ScSERF upon addition of pre-formed α-synuclein fibrils (F) and when competed against with unlabeled ScSERF (G).

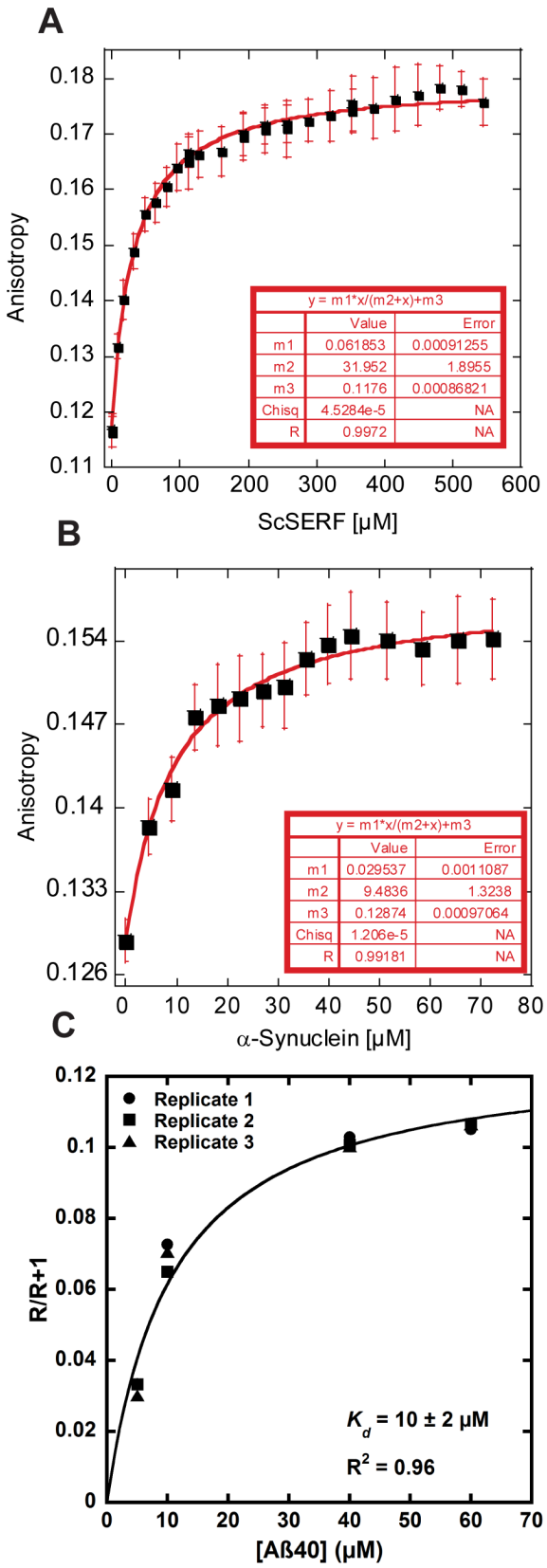
A
Anisotropy
ScSERF [μM]
y = m1*x/(m2+x)+m3
Value Error
m1 0.061853 0.00091255
m2 31.952 1.8955
m3 0.1176 0.00086821
Chisq 4.5284e-5 NA
R 0.9972 NA
B
Anisotropy
α-Synuclein [μM]
y = m1*x/(m2+x)+m3
Value Error
m1 0.029537 0.0011087
m2 9.4836 1.3238
m3 0.12874 0.00097064
Chisq 1.206e-5 NA
R 0.99181 NA
C
Replicate 1
Replicate 2
Replicate 3
R/R+1
[Aß40] (μM)
K_d = 10 ± 2 μM
R^2 = 0.96

Supplementary Figure 5 Binding constants for ScSERF binding to Aβ40/α-synuclein. (A) Increase in fluorescence anisotropy upon titration of ScSERF into monomeric AF532-labeled Aβ40. The equilibrium binding constant (K_d) was determined to be 31.9 ± 1.89 μM. Titration was performed at 25 °C in MS buffer (20 mM ammonium acetate, pH 7.4). (B) Increase in fluorescence anisotropy upon titration of α-synuclein into AF532-labeled ScSERF. The equilibrium binding constant (K_d) was determined to be 9.48 ± 1.32 μM. (C) 2 μM ScSERF was titrated with 5, 10, 40, and 60 μM Aβ40 to determine the dissociation constant (K_d) of ScSERF binding to monomeric Aβ40. At concentrations higher than 60 μM, Aβ40 was aggregating and thus interfering with accurate measurement of bound 1:1 ScSERF:Aβ40 complex. The response factor relationship of R/R+1 was plotted vs. Aβ40 concentration for 3 replicate measurements as described in the Materials & Methods. The data were fit using a quadratic function described previously for measuring K_d by MS (14). The data from 3 replicate measurements was fit with an R^2 of 0.96, and a K_d of 10 ± 2 μM was obtained.

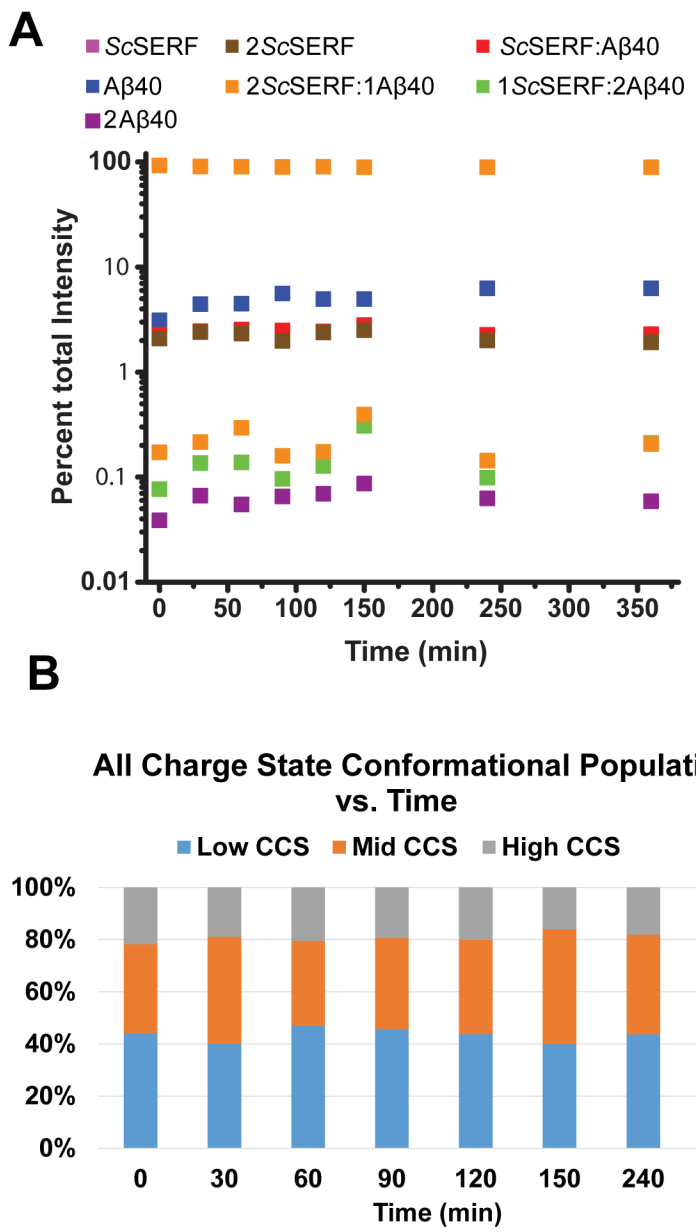

Supplementary Figure 6 Analysis of ScSERF interacting with Aβ40 overtime. Equimolar ratio of Aβ40:ScSERF were incubated at 37 °C in Corning, #3881 plate. Samples were taken at indicated time points and immediately analyzed by nESI-IM-MS. (A) Normalized Intensity of individual complexes observed over time. (B) From the IM-MS data, relative amount of different of 1:1 ScSERF:Aβ40 complex were monitored vs. time. The occupancy of each conformational state was determined by calculating the area under the Gaussian peaks fit to the raw data during collision cross section analysis. Overall, we found that the equilibria between complex stoichiometries, and the collision cross section populations was preserved over time.

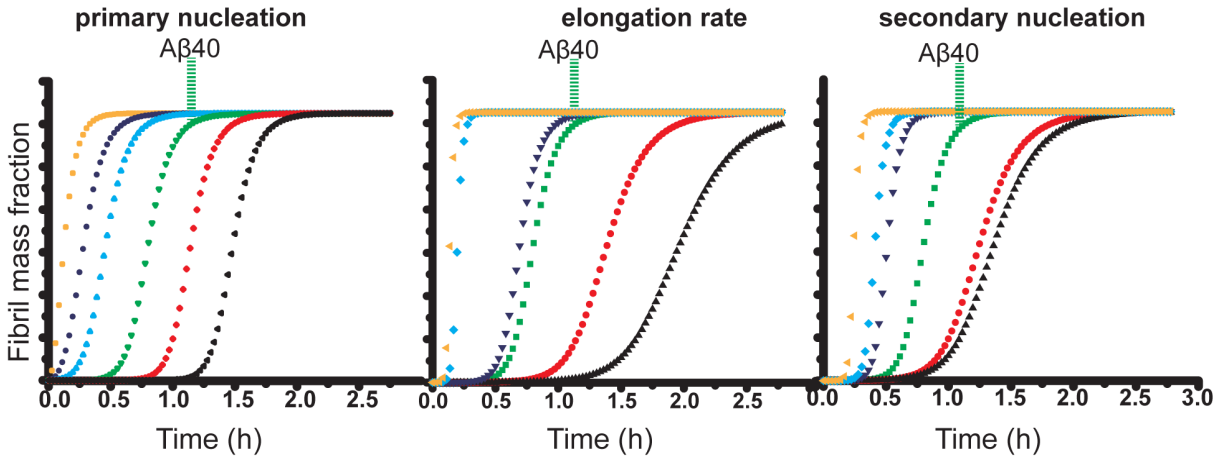

Supplementary Figure 7 Simulations showing the effect of changing the various rate constants on the kinetics of Aβ40 amyloid formation. Simulations of 25 μM Aβ40 were performed based on the published model (6, 9). For each set of curves, the result obtained using the published rate constants is shown in green (primary nucleation rate = 2×10^{-6}; elongation rate = 3×10^{5}, and secondary nucleation rate = 3×10^{3}); the other colored plots show how the aggregation curve's shape and lag time change by increasing or decreasing an individual rate constant. A change in elongation rate (middle set of curves) or secondary nucleation rate (right set of curves) not only changes the lag time, but also the shape of the curve. In contrast, changing the primary nucleation rate (left set of curves) only affects the lag time, consistent with our observed data.

Supplementary Table 1 Fitting parameters from fits in Fig. 1a

Aβ40:ScSERF	$k_n k_+$ [$M^{-1}s^{-1}$]	$k_+ k_2$ [$M^{-3/2}s^{-1}$]
1:0	7539.162559	1.94E+14
1:1	289758.5349	1.43E+14
1:0.5	800698.4702	1.85E+14
1:0.2	1820863.472	2.28E+14
1:0.1	13880596.78	2.05E+14

Supplementary Table 2 Primers for site-directed mutagenesis of ScSERF A63C and L9W

Forward A63C	5' GAAAAACTGGAAAAACTGAAATGTGAAAAAACCCGCCGCTAACTC 3'
Reverse A63C	5' GAGTTAGCGGCGGGTTTTTTCACATTTCAGTTTTTCCAGTTTTTC 3'
Forward L9W	5' CGGTAACCAGCGTGACTGGGCCCGTCAGAAAAATC 3'
Reverse L9W	5' GATTTTTCTGACGGGCCCAGTCACGCTGGTTACCG 3'

Supplementary References

1. Chen Y, et al. (2006) Crystal structure of human histone lysine-specific demethylase 1 (LSD1). *Proc Natl Acad Sci* 103(38):13956–13961.
2. Walsh DM, et al. (2009) A facile method for expression and purification of the Alzheimer's disease-associated amyloid β-peptide. *FEBS J* 276(5):1266–1281.
3. Jain N, Bhasne K, Hemaswasthi M, Mukhopadhyay S (2013) Structural and Dynamical Insights into the Membrane-Bound α-Synuclein. *PLoS One* 8(12):e83752.
4. Meisl G, Yang X, Dobson CM, Linse S, Knowles TPJ (2016) Molecular mechanisms of protein aggregation from global fitting of kinetic models. *Nat Protoc* 11(2):252–272.
5. Cohen SIA, et al. (2013) Proliferation of amyloid-β 42 aggregates occurs through a secondary nucleation mechanism. *Proc Natl Acad Sci* 110(24):9758–9763.
6. Meisl G, et al. (2014) Differences in nucleation behavior underlie the contrasting aggregation kinetics of the Aβ40 and Aβ42 peptides. *Proc Natl Acad Sci* 111(26):9384–9389.
7. Knowles TPJ, et al. (2009) An analytical solution to the kinetics of breakable filament assembly. *Science* 326(5959):1533–7.
8. Fairbanks G, Steck TL, Wallach DFH (1971) Electrophoretic analysis of the major polypeptides of the human erythrocyte membrane. *Biochemistry* 10(13):2606–2617.
9. Arosio P, et al. (2016) Kinetic analysis reveals the diversity of microscopic mechanisms through which molecular chaperones suppress amyloid formation. *Nat Commun* 7(1):10948.
10. Keith Richardson, David Langridge, Sugyan M. Dixit, Kevin Giles BTR (2019) An improved calibration approach for travelling wave ion mobility spectrometry: robust, high-precision collision cross sections. *Proceedings of the American Society of Mass Spectrometry Annual Conference*, p THP319.
11. Bush MF, et al. (2010) Collision Cross Sections of Proteins and Their Complexes: A Calibration Framework and Database for Gas-Phase Structural Biology. *Anal Chem* 82(22):9557–9565.
12. Haynes SE, et al. (2017) Variable-velocity traveling-wave ion mobility separation enhancing peak capacity for data-independent acquisition proteomics. *Anal Chem* 89(11):5669–5672.
13. Polasky DA, Dixit SM, Fantin SM, Ruotolo BT (2019) CIUSuite 2: Next-Generation Software for the Analysis of Gas-Phase Protein Unfolding Data. *Anal Chem* 91(4):3147–3155.
14. Ishii K, Noda M, Uchiyama S (2016) Mass spectrometric analysis of protein–ligand interactions. *Biophys Physicobiology* 13:87–95.